

# Ruthenium(II) Complex-Induced Dispersion of Montmorillonite in a Segmented Main-Chain Liquid-Crystalline Polymer Having Side-Chain Terpyridine Group

Wenyi Huang and Chang Dae Han\*

Department of Polymer Engineering, The University of Akron, Akron, Ohio 44325

Received August 24, 2006

Revised Manuscript Received October 13, 2006

Compatibility is one of the most important factors for achieving a very high degree of exfoliation of clay aggregates in a polymer matrix. Montmorillonite (MMT), which has widely been used to prepare polymer nanocomposites, is a type of smectic natural clay that tends to swell when exposed to water.<sup>1</sup> Thus, in its pristine state, MMT is only compatible with hydrophilic polymers, such as poly(ethylene oxide) (PEO)<sup>2</sup> or poly(vinyl alcohol) (PVA).<sup>3</sup> To render the compatibility between MMT and hydrophobic polymers, in most cases MMT was treated with a surfactant through ion-exchange reactions to convert the hydrophilic silicate surface into an organophilic one, and thus form the so-called organoclay.<sup>4–6</sup> A very high degree of exfoliation has seldom been observed in nanocomposites when there is little or no attractive interaction between the polymer matrix and MMT or organoclay. Therefore, one must design and synthesize a polymer such that the selected organoclay can have strong attractive interactions with the selected polymer.<sup>7,8</sup> The use of a ruthenium(II) complex for the preparation of a clay–metal complex hybrid film<sup>9</sup> or selective absorption onto clay surfaces has extensively been studied,<sup>10–13</sup> usually in connection with harnessing the specific interactions between metal-ion center and negatively charged clay surface.

In this study, we first synthesized a segmented main-chain liquid-crystalline polymer having side-chain terpyridine group (PTBP) and prepared a ruthenium complex [Ru<sup>II</sup>(PTBP)(6TPy)]-(PF<sub>6</sub>)<sub>2</sub> (referred to as PTBP–Ru–6TPy) by mixing PTBP with a monocomplex (6TPy–RuCl<sub>3</sub>), which was formed between a terpyridine (6-(2,2':6',2''-terpyridyl-4'-oxy)hexane (6TPy) and ruthenium chloride (RuCl<sub>3</sub>·3H<sub>2</sub>O). Subsequently, we prepared a (PTBP–Ru–6TPy)/MMT nanocomposite by solution blending. The MMT employed in this study has Na<sup>+</sup> ion, the ion-exchange capacity of 92 mequiv/100 g, and the dimensions of 1 nm in thickness, and approximately 100 nm in width and length. We found the MMT aggregates in the nanocomposite to be very well dispersed in the matrix of PTBP–Ru–6TPy. We attribute the very high degree of exfoliation of MMT aggregates observed to the Coulombic interactions between the negatively charged surfaces of pristine MMT and the positively charged ruthenium center in the polymer matrix. We are not aware of any previous study, which has reported on the formation of very high degree of exfoliation of pristine MMT aggregates in a polymer matrix having a metal complex.

Scheme 1 shows the reaction route employed to prepare ruthenium complex with PTBP, PTBP–Ru–6TPy, the detailed synthesis procedures and characterizations of which are summarized in the Supporting Information. Briefly stated, 6TPy was reacted with an equimolar amount of RuCl<sub>3</sub>·3H<sub>2</sub>O in methanol

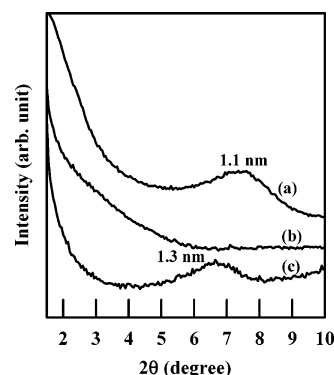


**Figure 1.** XRD patterns of (a) MMT, (b) (PTBP–Ru–6TPy)/MMT nanocomposite, and (c) PTBP/MMT nanocomposite.

at 60 °C overnight to form 6TPy–RuCl<sub>3</sub> monocomplex, which was further refluxed with PTBP in a cosolvent of tetrahydrofuran and ethanol (9:1, v/v), using *N*-ethylmorpholine as a catalyst, followed by the addition of an excess amount of ammonium hexafluorophosphate to finally obtain the PTBP–Ru–6TPy complex. It has been found from differential scanning calorimetry that PTBP has a glass transition temperature (*T*<sub>g</sub>) of 49.9 °C and a smectic-to-isotropic transition temperature of 80.7 °C during heating, while PTBP–Ru–6TPy only exhibits a *T*<sub>g</sub> of 123.4 °C upon heating (see the Supporting Information).

(PTBP–Ru–6TPy)/MMT nanocomposite was prepared by mixing a predetermined amount of PTBP–Ru–6TPy dissolved in a cosolvent of *N,N*-dimethylformamide (DMF) and H<sub>2</sub>O (10:1, v/v) and MMT aggregates suspended in a mixture of DMF and H<sub>2</sub>O (10:1, v/v) under vigorously stirring. The solvent in the mixture was evaporated slowly under constant stirring for 2 days at ambient temperature. When we prepared the (PTBP–Ru–6TPy)/MMT nanocomposite, the exchangeable interlayer cation Na<sup>+</sup> was exchanged by ruthenium complex in PTBP–Ru–6TPy and formed sodium hexafluorophosphate salt, which was still present in the final product.

For comparison, the PTBP/MMT nanocomposite was prepared using the same procedure, except that slight heating was applied to ensure the solubility of PTBP. Nanocomposites were dried completely in a vacuum oven at 100 °C until no weight change was detected. The amount of MMT (inorganic clay) in each nanocomposite (PTBP–Ru–6TPy)/MMT and PTBP/MMT was 3 wt %.

To determine the degree of dispersion of MMT aggregates in the nanocomposites, X-ray diffraction (XRD) experiments were conducted on a Rigaku Rotaflex rotating anode diffractometer with slit collimation. Figure 1 shows XRD patterns, showing that MMT has a gallery distance (*d*-spacing) of 1.1 nm, while the *d*-spacing of MMT in PTBP/MMT nanocomposite has increased only slightly from 1.1 to 1.3 nm, indicating that there would be little chance to obtain a highly dispersed MMT aggregates in PTBP. Interestingly, it can be seen in Figure 1 that (PTBP–Ru–6TPy)/MMT nanocomposite has a featureless XRD pattern, the origin of which can be attributed to the incorporation of ruthenium complex into PTBP that largely improves the compatibility between the MMT and the polymer. Transmission electron microscopy (TEM, JEM1200EX 11, JEOL) was conducted to verify the observations made from XRD patterns. It is clearly seen in Figure 2 that (PTBP–Ru–6TPy)/MMT nanocomposite has a very high degree of dispersion of MMT aggregates in the ruthenium complex matrix, while

\* To whom correspondence should be addressed. E-mail: cdhan@uakron.edu.

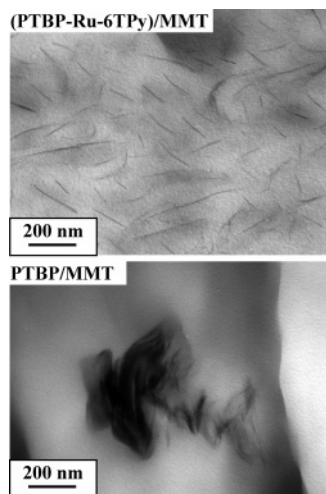


**Figure 2.** TEM images of (PTBP-Ru-6TPy)/MMT nanocomposite and PTBP/MMT nanocomposite, in which the dark areas represent the clay and the gray/white areas represent the polymer matrix.

PTBP/MMT nanocomposite has large aggregates of MMT, indicating poor dispersion of MMT aggregates.

Tris(2,2'-bipyridine)ruthenium(II) complex was reported to very selectively adsorb into the gallery of clay.<sup>10,11</sup> The evidence of strong interactions between the positively charged ruthenium center and the negatively charged clay surface is related to the red-shift of the positions of the metal-to-ligand charge-transfer band (MLCT) of tris(2,2'-bipyridine)ruthenium(II) complex and the decrease of the  $\pi-\pi^*$  band. In this study, the excellent ion-exchange property of ruthenium(II) complex was employed to exfoliate MMT aggregates in the polymer matrix. Figure 3 shows the ultraviolet-visible (UV-vis) spectra of thin films of PTBP-Ru-6TPy and (PTBP-Ru-6TPy)/MMT nanocomposite. It can be seen that the position of the MLCT band at a wavelength of about 493 nm for PTBP-Ru-6TPy has red-shifted to a wavelength of about 520 nm for (PTBP-Ru-6TPy)/MMT nanocomposite. The  $\pi-\pi^*$  band at a wavelength of 272 nm for PTBP-Ru-6TPy has decreased to a wavelength of 265 nm for (PTBP-Ru-6TPy)/MMT nanocomposite. The above observations are attributable to the Coulombic interactions

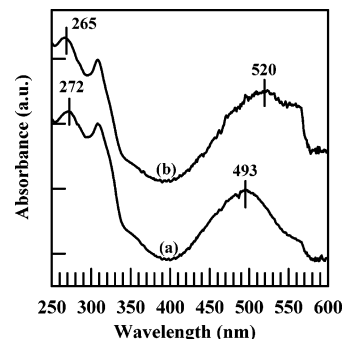


**Figure 3.** UV-vis spectra of thin films of (a) PTBP-Ru-6TPy and (b) (PTBP-Ru-6TPy)/MMT nanocomposite.

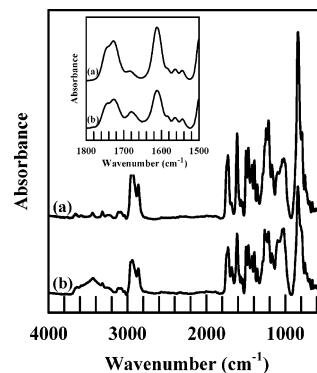
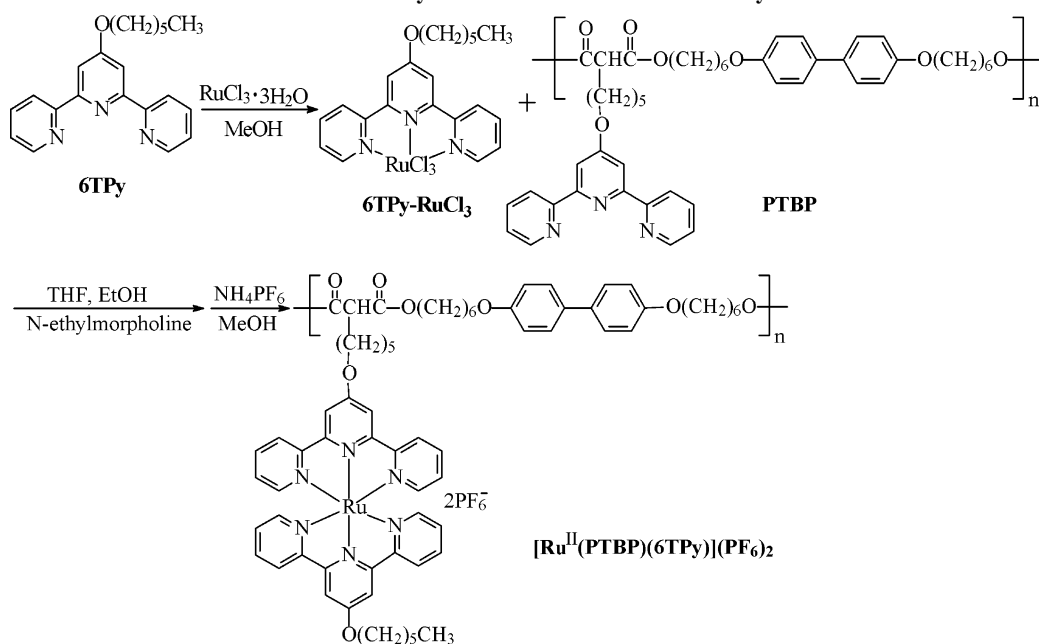


**Figure 4.** FTIR spectra of (a) PTBP-Ru-6TPy and (b) (PTBP-Ru-6TPy)/MMT nanocomposite. The inset shows the expanded absorption band at wavenumbers ranging from 1500 to 1800  $\text{cm}^{-1}$ .

between the positively charged ruthenium center and the negatively charged MMT surfaces, which are believed to be the driving forces that exfoliated MMT aggregates in the matrix of PTBP-Ru-6TPy. The Fourier transform infrared (FTIR) spectra shown in Figure 4 further confirm the presence of specific interactions, as evidenced by the increased intensity at a wavenumber of about 1680  $\text{cm}^{-1}$  (see the inset of Figure 4) and the new broad absorption peak appearing at a wavenumber of about 3420  $\text{cm}^{-1}$  for (PTBP-Ru-6TPy)/MMT nanocomposite. It should be mentioned that referring to the FTIR

#### Scheme 1. Synthesis Route for PTBP-Ru-6TPy



spectrum of pristine MMT shown in Figure 10a of the Supporting Information, the absorption peak at wavenumber  $3625\text{ cm}^{-1}$  originated from the O–H stretching of structural hydroxyl group, which is assigned to the hydroxyl groups coordinated to the octahedral cations, and the absorption peak at wavenumber  $3433\text{ cm}^{-1}$  originated from the H–OH hydrogen-bonded water.<sup>14–16</sup> When MMT was dispersed in PTBP–Ru–6TPy complex, the hydroxyl groups on the surface of MMT formed hydrogen bonds with the terpyridine groups in PTBP–Ru–6TPy complex. Thus, the absorption peak at  $3625\text{ cm}^{-1}$  for pristine MMT has been shifted to  $3420\text{ cm}^{-1}$  for (PTBP–Ru–6TPy)/MMT nanocomposite (see Figure 4). The absorption peak at  $1680\text{ cm}^{-1}$  (see the inset of Figure 4) is attributed to the ionization of terpyridine group and its strength is expected to increase in (PTBP–Ru–6TPy)/MMT nanocomposite due to the Coulombic interactions between the positively charged ruthenium center and the negatively charged MMT surface.

In this study, we also prepared two additional nanocomposites with PTBP–Ru–6TPy using two different organoclays, Cloisite 30B and Cloisite 15A, the surface of which has an organic surfactant (see the Supporting Information for details). The XRD patterns indicate that the *d*-spacing of Cloisite 30B aggregates in the (PTBP–Ru–6TPy)/(Cloisite 30B) nanocomposite has only increased from 1.9 to 4.4 nm, and the *d*-spacing of Cloisite 15A aggregates in the (PTBP–Ru–6TPy)/(Cloisite 15A) nanocomposite has only slightly increased from 3.1 to 3.5 nm. Correspondingly, (PTBP–Ru–6TPy)/(Cloisite 30B) nanocomposite has a flocculated dispersion, while (PTBP–Ru–6TPy)/(Cloisite 15A) nanocomposite exhibits an intercalated structure, as can be observed from TEM images. This suggests that the chance of direct interactions between the positively charged ruthenium center and the negatively charged MMT surfaces has been largely diminished, because of the shielding effect of the positively charged surfactants. It should be mentioned that in this study (PTBP–Ru–6TPy)/(Cloisite 30B) and (PTBP–Ru–6TPy)/(Cloisite 15A) nanocomposites were prepared by a simple mixing process.

In conclusion, here we have presented for the first time an experimental observation, in which ruthenium(II) complex in a functional liquid-crystalline polymer has exfoliated the pristine MMT aggregates through the Coulombic interactions between the positively charged ruthenium center and the negatively charged MMT surfaces. This observation provides a new

concept for molecular design to achieve a very high degree of dispersion of the aggregates of natural clay in the polymer matrix without the need to treat the natural clay with surfactant, and may pave a new way for preparing nanocomposites based on natural clay.

**Acknowledgment.** We acknowledge with gratitude that this study was supported in part by the National Science Foundation under Grant CST-04006752.

**Supporting Information Available:** Text giving detailed syntheses and characterizations of PTBP, 6TPy, and PTBP–Ru–6TPy and the preparation and characterizations of (PTBP–Ru–6TPy)/(Cloisite 30B) nanocomposite and (PTBP–Ru–6TPy)/(Cloisite 15A) nanocomposite including a scheme showing the synthesis routes for PTBP and  $[\text{Ru}^{\text{II}}(\text{PTBP})(6\text{TPy})](\text{PF}_6)_2$  and figures showing DSC thermograms, FTIR spectra, UV–vis spectra, XRD patterns, and TEM images. This material is available free of charge via the Internet at <http://pubs.acs.org>.

## References and Notes

- (1) Villemore, G. *Clays Clay Miner.* **1990**, *38*, 622.
- (2) Aranda, P.; Ruiz-Hizky, E. *Chem. Mater.* **1992**, *4*, 1395.
- (3) Greenland, D. J. *J. Colloid Sci.* **1963**, *18*, 647.
- (4) Fukushima, Y.; Okada, A.; Kawasumi, M.; Kurauchi, T.; Kamigaito, O. *Clay Miner.* **1988**, *23*, 27.
- (5) Usuki, A.; Kojima, Y.; Kawasumi, M.; Okada, A.; Kurauchi, T.; Kamigaito, O. *J. Mater. Res.* **1993**, *8*, 1179.
- (6) Usuki, A.; Kawasumi, M.; Kojima, Y.; Okada, A.; Kurauchi, T.; Kamigaito, O. *J. Mater. Res.* **1993**, *8*, 1174.
- (7) Huang, W.; Han, C. D. *Macromolecules* **2006**, *39*, 257.
- (8) Huang, W.; Han, C. D. *Polymer* **2006**, *47*, 4400.
- (9) Tamura, K.; Setsuda, H.; Taniguchi, M.; Yamagishi, A. *Langmuir* **1999**, *15*, 6915.
- (10) Schoonheydt, R. A.; Pauw, P. D.; Vliers, D.; Schrijver, F. C. D. *J. Phys. Chem.* **1984**, *88*, 5113.
- (11) Joshi, V.; Kotkar, D.; Ghosh, P. K. *J. Am. Chem. Soc.* **1986**, *108*, 4650.
- (12) Yamagishi, A.; Taniguchi, M.; Takahashi, M. *J. Phys. Chem.* **1994**, *98*, 7555.
- (13) Fujita, S.; Sato, H.; Kakegawa, N.; Yamagishi, A. *J. Phys. Chem. B* **2006**, *110*, 2533.
- (14) Tyagi, B.; Chudasama, C. D.; Jasra, R. N. *Spectrochim. Acta, Part A* **2006**, *64*, 273.
- (15) Esmer, K.; Tarken, E. *Spectroscopy Lett.* **2001**, *34*, 443.
- (16) Katti, K. S.; Sikdar, D.; Katti, D. R.; Ghosh, P.; Verma, D. *Polymer* **2006**, *47*, 403.

MA0619637